

doi:10.15199/48.2022.06.22

Performances comparison of BLDC and BLAC motors based matrix converter

Abstract. The ability to adjust the speed of a brushless motor is widely used in a variety of applications. Because of its great energy density, efficiency, and resilience, it is recommended. On the other hand, the matrix converter (MC) is an AC / AC power supply system which has many advantages which allow to maintain the quality of the energy supplied directly from the network more efficient and well filtered. This article proposes a comparative study of the speed control of a brushless motor supplied first through an inverter and then directly from the grid using a matrix converter in terms of power quality performances and cost.

Streszczenie. Możliwość regulacji prędkości silnika bezszczotkowego jest szeroko stosowana w różnych zastosowaniach. Ze względu na dużą gęstość energii, wydajność i odporność jest polecana. Z kolei konwerter macierzowy (MC) to system zasilania AC/AC, który ma wiele zalet, które pozwalają na utrzymanie jakości energii dostarczanej bezpośrednio z sieci bardziej wydajnej i dobrze filtrowanej. W artykule zaproponowano badanie porównawcze regulacji prędkości obrotowej silnika bezszczotkowego zasilanego najpierw przez falownik, a następnie bezpośrednio z sieci za pomocą przekształtnika macierzowego pod względem wydajności i kosztów. (Porównanie wydajności konwertera matrycowego opartego na silnikach BLDC i BLAC)

Keywords: BLDC motor, matrix converter, SVM method, PI.

Słowa kluczowe: Silnik BLDC, przetwornik matrycowy, metoda SVM, PI.

Introduction

During the 1960s, the development of semiconductor components led to the invention of the first brushless direct current (BLDC) motor in 1962. BLDC motor is the inside-out DC motor where the three-phase armature windings are mounted on the stator, and the rotor consists of permanent magnets resembling the mechanical structure of a permanent magnet brushed dc motor (PMDCM) except the brushes required for commutation [1].

The stability of the BLDC speed allows the motor to produce a desired high torque. Conventional control techniques such as Proportional-integral-derivative (PID) or proportional-integral (PI) were used widely in the field of BLDC speed control addressing to the converter control part [2].

In this context, matrix converters (MCs) are one of the most attractive families of converters in the power electronics field. The progress of this converter started in the 1980s. Hence we have the possibility of having a detailed mathematical model to describe the low-frequency operation of this converter [3].

In this paper, a study of a proposed control of the speed of BLDC motor supplied directly from the grid using a Matrix Converter is compared with the classical PI control.

1. Brushless motors

BLDC motor is considered to be asynchronous motor with a permanent magnet [1, 4] and has become today a tool indispensable in various applications thanks to its superior performance [5, 6].

BLDC motor takes its name instead of the current motor, which has windings on the rotor and requires a collector to supply these windings. This collector is a weak point of the direct current motor: energy losses (mechanical and electrical), wear, sparks, etc. [2, 7].

Brushless motors have a lot of advantages over DC motors: the absence of brushes leads to better energy performance and better reliability [2]. With the windings being on the stator, the heat dissipation is more straightforward and the inertia is reduced (the copper windings on the rotor of DC motors are very heavy), which further improves energy performance in applications requiring accelerations and decelerations [1, 8]. The

weight/power ratio is better, and the cost of electronic controls three-phase is now less than the cost of a collector [9, 10]. For specialized applications, the synchronous machine control allows precise control of the magnetic field in the machine, and thus the torque generated, much better than on a DC motor. Also, the brushless motor is gradually replacing the DC motor in some fields application, in particular when the mass or the speed of rotation are important criteria [11].

1.1 Operation principle of brushless motors

Among synchronous machines, the self-controlled synchronous machine corresponds to the brushless motor with sinusoidal control (BLAC, Brushless Alternative Current), while the BLDC motor (Brushless Direct Current) corresponds to a brushless motor controlled by niche.

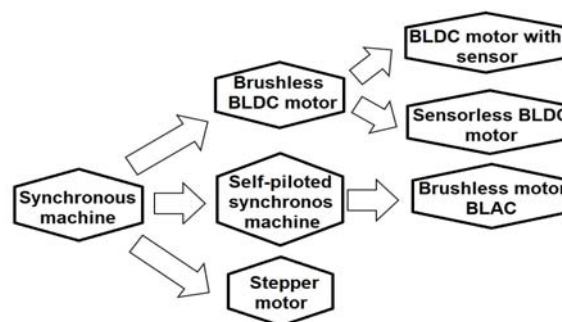


Fig.1. Synchronous machine type

In the case of the BLCD, the switching can be controlled from measurement by sensors at Hall effect at 6 points per revolution, or even from a counter-electromotive force measurement (motors known without sensors: "sensorless")[4, 12].

2. The matrix converter

CM is a new topology of the direct frequency converters. It allows to have a system of voltages variable in amplitude and frequency from the fixed voltages of the electrical network [13- 15]. This is achieved using a matrix of

bidirectional power switches, in voltage and current, connecting each input phase to each output phase [16]. We are talking about a direct conversion frequency because the conversion is performed without an intermediate circuit (DC-DC bus), allowing energy storage [13- 17]. In fact, it has many advantages compared to its multistage counterparts, such as its compact size [18], low weight, and bulk, high power density, and reliability [19, 20].

Until today, CM has been used in industrial sectors such as wind power generation. However, the control of these systems still remains face several challenges, such as network imbalance, harmonics, drops in voltage and disturbances [20, 21]. Several modulation techniques have been reported such as the pulse width modulation of the spatial vector, the scalar modulation method and the Venturini modulation method [19, 22].

2.1 Advantages and disadvantages of CM

The following points describe the advantage of CM:

- Wide range of output frequencies and high power density [23].
- The power factor at the output varies depending on the operating point of the load, and for the input power factor, it can be unitary.
- The power factor at the input can be unitary. Moreover it can be imposed by control; this is, however linked to a decrease in the maximum voltage of the output, which decreases with the cosine of the phase shift [20].
- The input currents are almost sinusoidal [24, 25].
- We can work in both directions therefore, in the four quadrants of the current-voltage plane [22, 26].

And as disadvantages of this converter, we have:

- A large number of switches [27].
- The sensitivity of switches to external disturbances.
- The more complicated ordering system [27].

2.2 Operation principle of CM

A matrix converter consists of nine bidirectional voltage switches and by current connecting three input phases to that of the load [22]. A low pass filter must be placed at the input of the CM, whose objective is to thwart the propagation of harmonic currents in the electrical network [28].

2.3 CM Switches

Elementary elements (Diodes, thyristors, IGBTs, MOSFETs, etc.) must be associated to have a bidirectional switch for voltage and current [29].

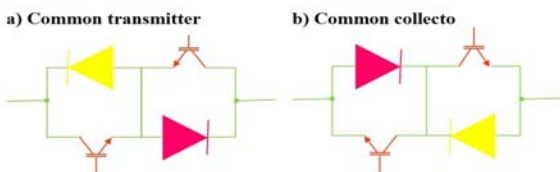


Fig.2. Structures of bidirectional switches with 2 IGBTs and diodes in series

The bidirectional switch with a common emitter (Figure 2 (a)) has two diodes. The objective is to ensure reverse blocking and two IGBTs [30]. These two components are connected in antiparallel. There are several advantages to using this switch; the first advantage is that it is possible to independently control the current direction. The second advantage is the conduction losses, which are reduced because only two devices carry the current at all times [30].

The bidirectional switch with the common collector is identical to that of Figure 2 (b); except that in practice, this type of switch is not feasible, and this is due to the presence of parasitic inductance between the switching cells, which causes problems troublesome [30-32].

2.4 Protection circuit

The switching strategies applied to the CM require the measurement of the currents of output. This measurement is carried out using a Hall effect sensor or shunt. The precision of measuring devices leads, for low currents, to a possible error on their sign and thus to overvoltages due to openings of these currents out of time.

In fact, we can use a clamping circuit (Clamping) shown in Figure 3 to protect the converter against these overvoltages. When the diode rectifier bridge is located between the three-phase network and the load, the DC capacitor is subjected to phase-to-phase voltages greater than the peak phase-to-phase voltages of the CM at the output. In this case, the diode rectifier bridge will not conduct. If the output voltages exceed this value, the corresponding bridge connects the output terminals to the capacitor and limits the voltage to the voltage value across the capacitor. This clipping system protects the CM overvoltages coming from the network and those coming from a sudden disconnection of the charge [33].

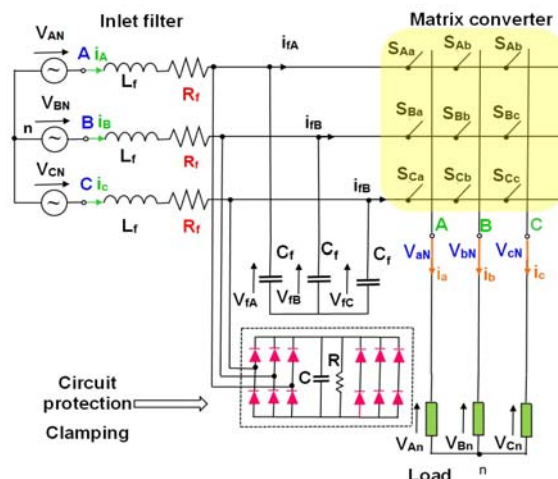


Fig.3. Block diagram of a CM with a protection circuit (Clamping)

3. Modeling of the system

3.1 Modeling of the BLDC

Typically brushless direct current (BLDC) motors have a star-coupled stator winding. The BLDC motor winding feed will be in appropriate sequences. Figure 4 presents the operating principle of a BLDC machine.

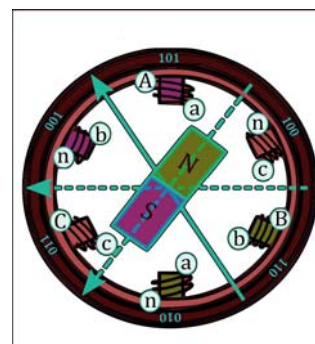


Fig.4. Operating principle of a BLDC machine

Depending on the shape of the back electromotive force (FEM), there are two types of BLDC motors: sinusoidal and trapezoidal. Figure 5 presents an example of a back-EMF and optimal current profiles in each phase together with Hall sensor signals.

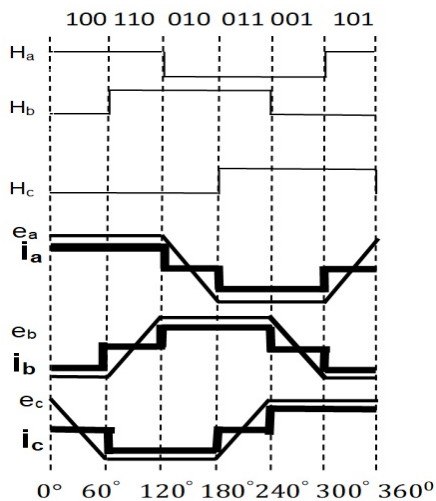


Fig.5. Back-EMF and optimal current profiles in each phase together with Hall sensor signals

a. Electrical equations:

The equations electric that govern engine operation BLDC are given by the following equations:

$$(1) \quad \vec{V} = [R]\vec{I} + \frac{d\vec{\varphi}}{dt}$$

$$(2) \quad \vec{\varphi} = [R]\vec{I} + \vec{\varphi}_M$$

\vec{V} \vec{I} $\vec{\varphi}$ are vectors representing the voltage, the current and magnetic flux for each phase respectively.

$\vec{\varphi}_M$: is the vector of the magnetic flux.

$[R]$ et $[L]$ are the resistance and inductance matrices of the machine given by the following matrices:

$$(3) \quad R = \begin{bmatrix} R & 0 & 0 \\ 0 & R & 0 \\ 0 & 0 & R \end{bmatrix}$$

$$(4) \quad L = \begin{bmatrix} L_a & L_{ab} & L_{ac} \\ L_{ba} & L_b & L_{bc} \\ L_{ca} & L_{cb} & L_c \end{bmatrix}$$

When the motor is star-coupled, the phase voltages take the following form:

$$(5) \quad \begin{bmatrix} V_a \\ V_b \\ V_c \end{bmatrix} = \begin{bmatrix} R & 0 & 0 \\ 0 & R & 0 \\ 0 & 0 & R \end{bmatrix} \begin{bmatrix} i_a \\ i_b \\ i_c \end{bmatrix} + \begin{bmatrix} L-M & 0 & 0 \\ 0 & L-M & 0 \\ 0 & 0 & L-M \end{bmatrix} \frac{d}{dt} \begin{bmatrix} i_a \\ i_b \\ i_c \end{bmatrix} + \begin{bmatrix} e_a \\ e_b \\ e_c \end{bmatrix}$$

$$(6) \quad e_a = K_a \omega_m \cos \theta t$$

$$(7) \quad e_b = K_b \omega_m \left(\cos \theta t - \frac{2\pi}{3} \right)$$

$$(8) \quad e_c = K_c \omega_m \left(\cos \theta t - \frac{2\pi}{3} \right)$$

b. Mechanical equation:

The mechanical model of the BLDC motor is more straightforward than the electric model. Indeed, the modeling of the rotor dynamics is standard in the field of electric machines.

The following equation defines the dynamics of the rotor:

$$(9) \quad J \frac{\omega_m}{dt} = t_{em} - t_L - F_{om}$$

$$(10) \quad t_{em} = \frac{1}{\omega_m} (e_a i_a + e_b i_b + e_c i_c)$$

$$(11) \quad \omega = P_{\omega_m}$$

3.2 Modeling of the CM

To establish the relations associating the quantities of entry and exit of the CM, one takes into account the power supply network and the input filter. We have a pure three-phase voltage source so that at the output, we have an ideal current source. In the same way, we pose that the switches are ideal: we neglect their leakage currents in the blocked state and their drops voltage in the conduction state, and it is estimated that the commutations are instantaneous.

Thus, the CM appears as a non-energetic connection multipoint. In this case, we can characterize the state of each switch by a logic variable equal to 1 if the switch is conductive and 0 if it is blocked.

For example, for the switch \vec{S}_{ij} which gives the possibility of connecting the input terminal i at the output terminal j , we have:

$$S_{ij} = \begin{cases} 1 & \text{if switch } \vec{S}_{ij} \text{ is closed} \\ 0 & \text{if switch } \vec{S}_{ij} \text{ is open} \end{cases}$$

With: $i = \{A, B, C\}$ and $j = \{a, b, c\}$

The instantaneous three-phase input and output voltages are written in the form matrix:

$$(12) \quad V_{ec} = \begin{bmatrix} V_{AN} \\ V_{BN} \\ V_{CN} \end{bmatrix}; V_{SC} = \begin{bmatrix} V_{an} \\ V_{bn} \\ V_{cn} \end{bmatrix}$$

From Figure 3, the input and output relationship can be represented as a matrix by:

$$(13) \quad \begin{bmatrix} V_{an} \\ V_{bn} \\ V_{cn} \end{bmatrix} = \begin{bmatrix} S_{Aa} & S_{Ba} & S_{Ca} \\ S_{Ab} & S_{Bb} & S_{Cb} \\ S_{Ac} & S_{Bc} & S_{Cc} \end{bmatrix} \begin{bmatrix} V_{AN} \\ V_{BN} \\ V_{CN} \end{bmatrix}$$

We can also express the relation (13) by the form:

$$(14) \quad V_{SC} = S \cdot V_{ec}$$

With S : The instantaneous transfer matrix.

The phase-to-phase voltages at the output of the CM are expressed by the following form:

$$(15) \quad \begin{cases} V_{ab} = V_{an} - V_{bn} = S_{Aa}V_{AN} + S_{Ba}V_{BN} + S_{Ca}V_{CN} - S_{Ab}V_{AN} - S_{Bb}V_{BN} - S_{Cb}V_{CN} \\ V_{bc} = V_{bn} - V_{cn} = S_{Ab}V_{AN} + S_{Bb}V_{BN} + S_{Cb}V_{CN} - S_{Ac}V_{AN} - S_{Bc}V_{BN} - S_{Cc}V_{CN} \\ V_{ca} = V_{cn} - V_{an} = S_{Ac}V_{AN} + S_{Bc}V_{BN} + S_{Cc}V_{CN} - S_{Aa}V_{AN} - S_{Ba}V_{BN} - S_{Ca}V_{CN} \end{cases}$$

We can write the equation (15) by the following form:

(16)

$$\begin{bmatrix} V_{ab} \\ V_{bc} \\ V_{ca} \end{bmatrix} = \begin{bmatrix} (S_{Aa} - S_{Ab}) & (S_{Ba} - S_{Bb}) & (S_{Ca} - S_{Cb}) \\ (S_{Ab} - S_{Ac}) & (S_{Bb} - S_{Bc}) & (S_{Cb} - S_{Cc}) \\ (S_{Aa} - S_{Aa}) & (S_{Bc} - S_{Ba}) & (S_{Cc} - S_{Ca}) \end{bmatrix} \begin{bmatrix} V_{AN} \\ V_{BN} \\ V_{CV} \end{bmatrix}$$

The relation between the instantaneous input currents and those of the output

$$(17) \quad \begin{bmatrix} I_A \\ I_B \\ I_C \end{bmatrix} = \begin{bmatrix} S_{Aa} & S_{Ab} & S_{Ac} \\ S_{Ba} & S_{Bb} & S_{Bc} \\ S_{Ca} & S_{Cb} & S_{Cc} \end{bmatrix} \begin{bmatrix} I_a \\ I_b \\ I_c \end{bmatrix}$$

We can also express the relation (17)

$$(18) \quad I_{ec} = S^t \cdot I_{sc}$$

With S_t is the transposed matrix of S .

$$(19) \quad I_{ec} \begin{bmatrix} I_A \\ I_B \\ I_C \end{bmatrix}; I_{sc} \begin{bmatrix} I_a \\ I_b \\ I_c \end{bmatrix}$$

The switches of the same column must be complementary so that the voltage source is never in a short circuit and so that the load is never an open circuit. In that case, we have:

$$(20) \quad S_{Aj} + S_{Bj} + S_{Cj} = 1$$

Therefore, the CM has 27 possible combinations of commutations.

We suppose that $t_{ij}(t)$ the conduction duration of the switch S_{ij} is defined by the following relation:

$$(21) \quad T_{Aj} + T_{Bj} + T_{Cj} = T_{seq}$$

Where : T_{seq} : The period or the switching sequence of the CM.

In this case:

$$0 < T_{ij} < T_{seq}$$

We suppose that $m_{ij}(t)$ is the conduction duty cycle of

the interceptor S_{ij} , defined by:

$$(22) \quad m_{ij}(t) = \frac{t_{ij}}{T_{seq}}$$

The duty cycle $m_{ij}(t)$ of the switches S_{ij} with the switching period T_{seq} is represented by the following relation:

$$(23) \quad m_{ij}(t) = \frac{t_{ij}}{T_{seq}} = \int_0^{T_{seq}} S_{ij}(t) dt$$

Avec $0 < m_{ij} < 1$

On the other hand and according to equation (23), we can write:

$$(24) \quad m_{Aj} + m_{Bj} + m_{Cj} = 1$$

We have:

$$(25) \quad \begin{bmatrix} V_{an} \\ V_{bn} \\ V_{cn} \end{bmatrix} = \begin{bmatrix} m_{Aa} & m_{Ba} & m_{Ca} \\ m_{Ab} & m_{Bb} & m_{Cb} \\ m_{Ac} & m_{Bc} & m_{Cc} \end{bmatrix} \begin{bmatrix} V_{AN} \\ V_{BN} \\ V_{CV} \end{bmatrix}$$

$$(26) \quad \begin{bmatrix} I_A \\ I_B \\ I_C \end{bmatrix} = \begin{bmatrix} m_{Aa} & m_{Ab} & m_{Ac} \\ m_{Ba} & m_{Bb} & m_{Bc} \\ m_{Ca} & m_{Cb} & m_{Cc} \end{bmatrix} \begin{bmatrix} I_a \\ I_b \\ I_c \end{bmatrix}$$

Where M : The modulation matrix.

$$(27) \quad M = \begin{bmatrix} m_{Aa} & m_{Ba} & m_{Ca} \\ m_{Ab} & m_{Bb} & m_{Cb} \\ m_{Ac} & m_{Bc} & m_{Cc} \end{bmatrix}$$

3.3 Modeling of the the SVM method

The SVM strategy represents three-phase input currents and phase-to-phase voltages the output of the spatial vectors V_S . It is based on the concept approximation of a reference voltage vector in rotation with these voltages, which are physically achievable on a matrix converter. For the nine bidirectional switches, there are 27 possible switching combinations, of which there are only 21 which are commonly used to generate the space vectors to achieve this SVM command. The first three groups ($\pm 1, \pm 2, \pm 3, \pm 4, \pm 5, \pm 6, \pm 7, \pm 8, \pm 9$) have two common characteristics; namely: each of them consists of six vectors that keep the angular positions constant, and each of them forms a hexagon of sextant.

The general formulas allowing to calculate the duration of activation time of switches are presented by the following expressions [34, 35]:

$$(28) \quad \delta_1 = \frac{2}{\sqrt{3}} q \sin \left[\varphi_{sc} - (k_s - 1) \frac{\pi}{3} \right] \sin \left[\frac{\pi}{6} - (\varphi_{ec} - (k_e - 1)) \frac{\pi}{3} \right]$$

$$(29) \quad \delta_2 = \frac{2}{\sqrt{3}} q \sin \left[\varphi_{sc} - (k_s - 1) \frac{\pi}{3} \right] \sin \left[\frac{\pi}{6} + (\varphi_{ec} - (k_e - 1)) \frac{\pi}{3} \right]$$

$$(30) \quad \delta_3 = \frac{2}{\sqrt{3}} q \sin \left[k_s \frac{\pi}{3} - \varphi_{sc} \right] \sin \left[\frac{\pi}{6} - (\varphi_{ec} - (k_e - 1)) \frac{\pi}{3} \right]$$

$$(31) \quad \delta_4 = \frac{2}{\sqrt{3}} q \sin \left[k_s \frac{\pi}{3} - \varphi_{sc} \right] \sin \left[\frac{\pi}{6} + (\varphi_{ec} - (k_e - 1)) \frac{\pi}{3} \right]$$

The switching laws are respected by adding the duty cycle of a zero-configuration δ_0 :

$$(32) \quad \delta_0 = 1 - (\delta_1 + \delta_2 + \delta_3 + \delta_4)$$

Determination of the cyclic ratios m_{ij} of the switches is done from the ratios δ_i , the most straightforward strategy to do is to sum the four ratios δ_i of the four shapes defined during a sampling instant.

$$(33) \quad \begin{cases} T_{Aa} + T_{Ab} + T_{Ac} = T_{seq} \\ T_{Ba} + T_{Bb} + T_{Bc} = T_{seq} \\ T_{Ca} + T_{Cb} + T_{Cc} = T_{seq} \end{cases}$$

Finally, we list the function of each switch on an instant. Sampling. Its duty cycle m_{ij} is equal to the sum of the ratios δ_i of configurations to which it belongs. The selection allows us to assign different configurations and which gives us other values for cyclic ratios m_{ij} .

The modulation strategy provided will generate the control pulses, which will be sent to the gates of the transistors. It is simply necessary to confront the m_{ij} sawtooth signal control algorithm calculated where the base is equal to the sampling instant and whose amplitude is unitary.

In fact, a 256 level sawtooth signal can be quickly produced by a clock, an 8-bit counter, and a N/A converter. Regarding SVM, we join in the literature of other double-slope methods, and these methods seek to characterize a way to apply the selected configurations and to place the zero configurations to optimize the quality of the waves produced by the CM [36].

3.4 Sizing the inlet filter

The sizing of the filter meets the following technical specifications:

- The harmonics at the pulse frequency of the input current of the CM are sufficiently well-damped against the input current of the filter. This will be determined by the function $F_2(p)$ which is taken from equation (34):

$$(34) \quad F_2(p) = \frac{1}{L_f C_f} \frac{1}{p^2 + \frac{R_f}{L_f} p + \frac{1}{L_f C_f}}$$

- The voltage across the inductance of the filter L_f remains within several limits under the influence of pulsation. There should be no overvoltage pulses that prevent high current switching by the CM. The impulses of

power surges can destroy switches. This is imposed by the functions $F_1(p)$ and $F_3(p)$ which are taken from equations (35) and (36) respectively [37]:

$$(35) \quad F_1(p) = \frac{C_f p}{L_f C_f p^2 + R_f C_f p + 1}$$

$$(36) \quad F_3(p) = R_f + L_f p$$

- The input power factor is not too small. The filter will cause a displacement between the fundamental signals of network voltage and current, decreasing the power factor [38].

- It is recommended that the values of components, in particular capacitors, are as small as possible.

For the sizing of the input filter, it is first necessary to choose the frequency of resonance f_0 , this choice will be essentially determined by the pulse frequency of the CM and the spectrum of harmonics of the input current [37].

With the neglect of the resistance R_f , the equation (37)

of $F_2(p)$ can be rewritten in the frequency domain:

$$(37) \quad |F_2(\omega)| \approx \frac{\omega_0}{\sqrt{\omega_p^2 - \omega_0^2}}$$

When the pulse frequency is higher, the resonant frequency of the filter is higher and therefore the values of the passive elements will be smaller, this frequency is given by equation (38):

$$(38) \quad f_0 = \frac{1}{2\pi L_f C_f}$$

This type of input filter has an amplitude equal to Q_0 defined in (39):

$$(39) \quad Q_0 = \frac{1}{R_f} \sqrt{\frac{L_f}{C_f}}$$

We can choose the pulse ω_0 according to:

$$(40) \quad \omega_0 = 2\pi f_0 = \omega_p \frac{\sqrt{Q_p}}{\sqrt{Q_p + 1}}$$

With Q_p is the gain at the pulse frequency ω_p .

The cutoff frequency f_p is determined by the relation (41):

$$(41) \quad f_p = \frac{\sqrt{2}}{2\pi L_f C_f}$$

Then, there remains only one parameter to determine, the weighting between the component capacitive and the inductive component. As a criterion for this, one can choose one among the last three criteria which were set before for the characteristics of the filter. If we size the filter by limiting the amplitudes of the harmonics of the output voltage, the determining transfer function is given by the product of the functions $F_2(p)$ and $F_3(p)$; By rewriting the function

$F_3(p)$ in the frequency domain also with the neglect of the resistance R_f , we will have:

$$(42) \quad |F_3(\omega)| = L_f \omega_p$$

And so:

$$(43) \quad Q_p = |F_2(\omega)| |F_3(\omega)| = \frac{L_f \omega_0 \omega_p}{\sqrt{\omega_p^2 - \omega_0^2}}$$

With Q_p is the ratio of the voltage harmonics introduced by the pulsation, the reactance L_f with respect to the pulsation frequency is represented by the following formula:

$$(44) \quad L_f = \frac{Q_p \sqrt{\omega_p^2 - \omega_0^2}}{\omega_0 \omega_p}$$

This strategy is well used for determining the minimum capacity required choose to ensure the safe operation of the drive system appearance of surges.

According to Bode's diagram, the function $F_2(p)$ introduces the unity gain and the phase shift disappears at nominal frequency.

By rewriting the function $F_1(p)$ in the frequency domain, we will have:

$$(45) \quad |F_1(P)| = \frac{1}{L_f} \frac{\omega_0 \omega_p}{\sqrt{\omega_p^2 - \omega_0^2}}$$

4. Simulation results and discussions

4.1. BLDC motor driven by a DC / AC converter

on first place; we will study the operation of a BLDC motor driven through an inverter as shown in the figure 6; at $t = 0.15$, a load torque of 4 N.m is applied

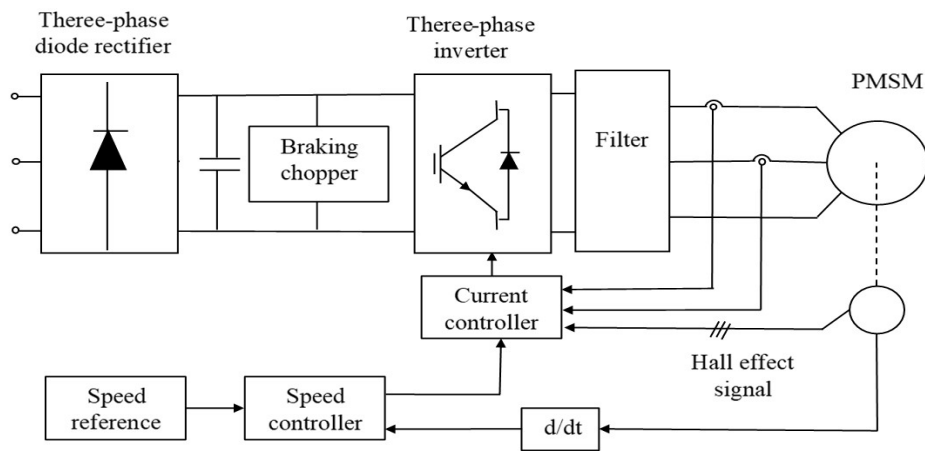


Fig.6. BLDC motor fed with indirect matrix converter

Table 1. The parameters of the motor

Stator phase resistance R_s (ohm)	2.8750
Stator phase inductance (H)	$8.5e^{-5}$
Flux linkage	0.175
Voltage constant	146.6077
Torque constant	1.4
Back EMF flat area (degrees)	120

The electromagnetic torque of the BLDC motor is represented by the figure 7 where at $t = 0.1 \text{ s}$, we notice the variation of the torque from 0 to 4 N.m with the presence of some overshoot

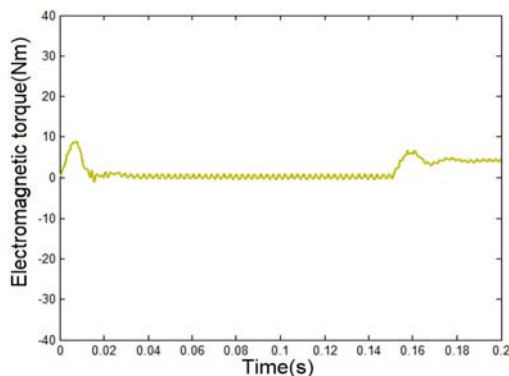


Fig.7. The electromagnetic torque

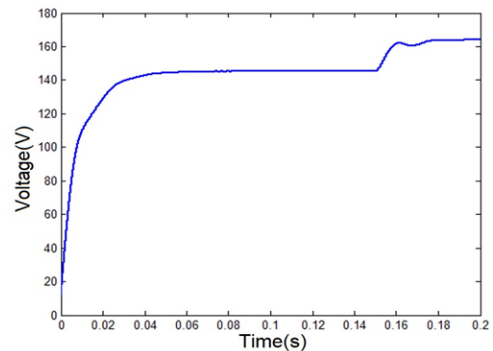


Fig.8. DC link voltage

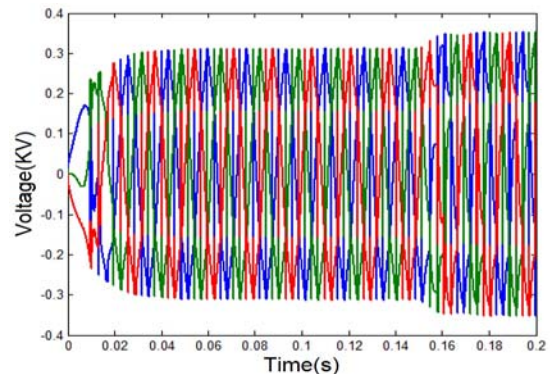


Fig.9. The simple voltages

Figure 8 describes the DC link voltage of the inverter through the control of the inverter switches; we obtain the form of the three-phase simple voltages mentioned in figure 9. The line voltage is shown in the figure 10

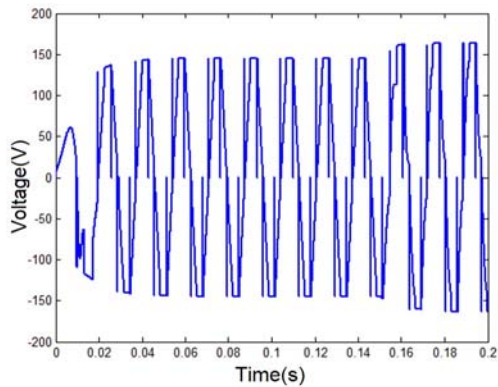


Fig.10. the line voltage

the figure11 describes the current of the BLDC motor. After the current passes through the output filter of the inverter; we get the shape of the figure

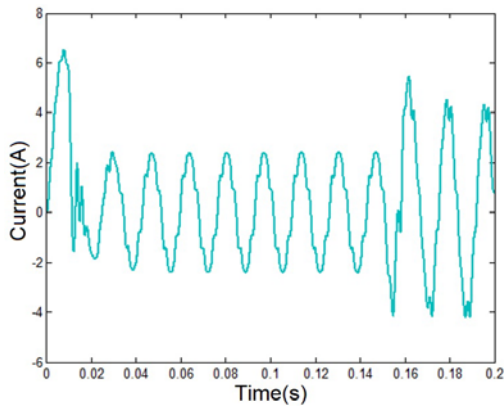


Fig.11. Stator current

figure 12 describes the spectral analysis of the current, which is characterized by a harmonic distortion rate of 15.28%

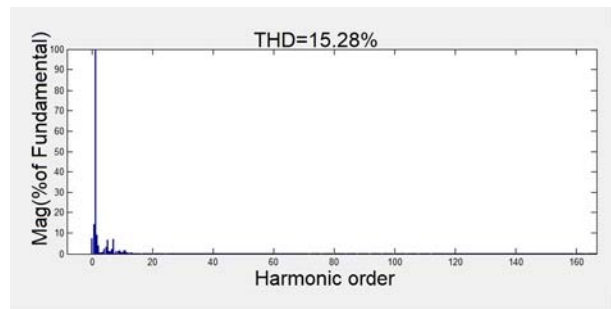


Fig.12. Stator current spectrum

The motor control makes it possible to stabilize the speed value after the variation of the torque with some overshoots.

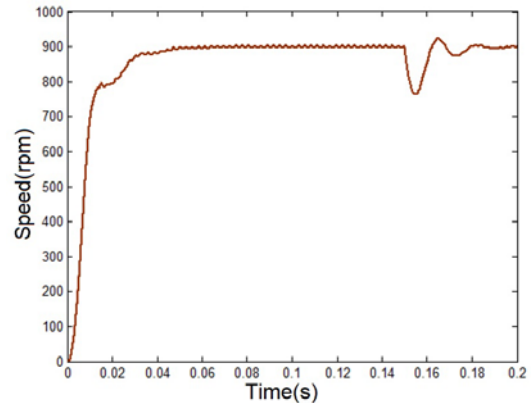


Fig.13. The motor speed

The electromotive force of the motor is mentioned in figure 14

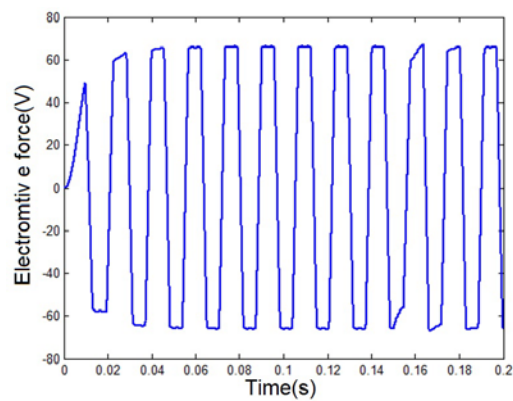


Fig.14. electromotive force

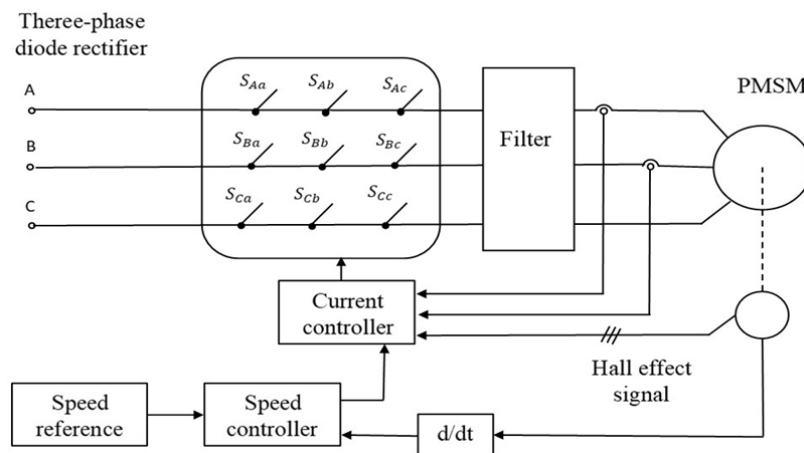


Fig.15. BLDC motor fed with matrix converter

4.2. BLDC motor driven through an AC / AC converter

In this part, we replace the DC / DC converter with a direct matrix converter, as shown in figure 15. We apply the same previous conditions

Figure 16 describes the shape of the electromagnetic torque after the torque variation. The force takes its stability, the source voltage is shown in the figure 17

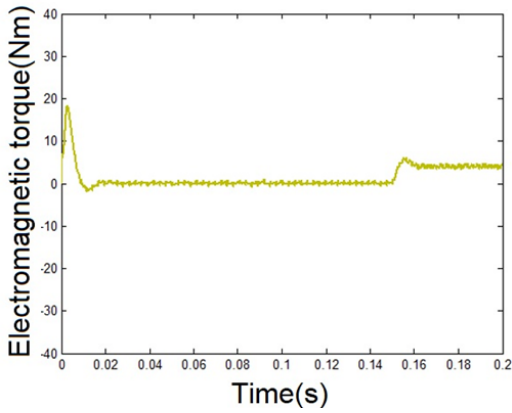


Fig.16. Electromagnetic torque

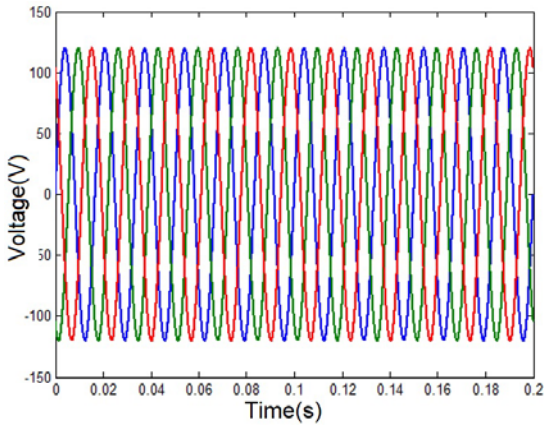


Fig.17. Source voltage

The converter voltages are written in the figure 18, where the form of the line voltage is mentioned in the figure 19

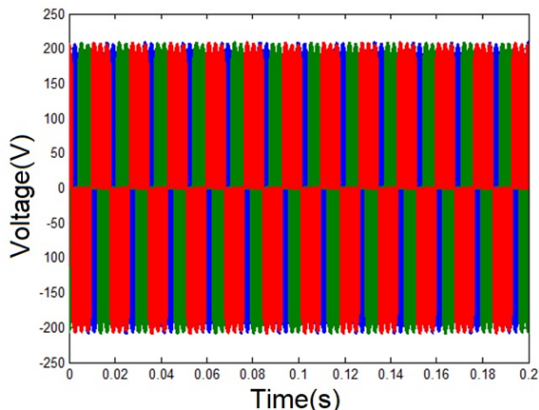


Fig.18. Charging voltage

Figure 20 shows the form of the motor current. It can notice that it is smooth sinusoidal, which is reflected by the spectral analysis of figure 21, which shows a significantly reduced rate of the presence of harmonics of 2.88 %

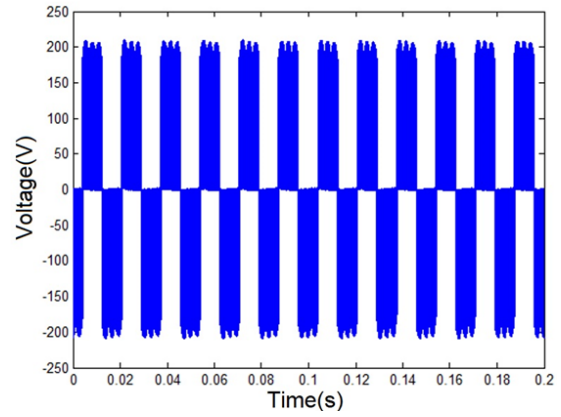


Fig.19. Vab motor

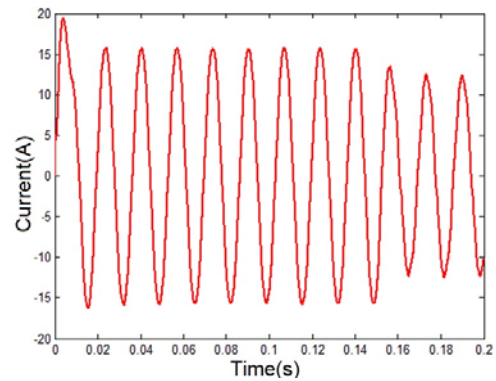


Fig.20. Stator current

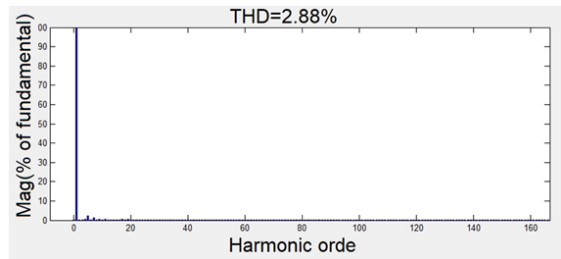


Fig.21. Stator current spectrum

The motor speed is present by overshoot after the torque variation

It takes its stability directly as shown in figure 22, which gives a stable electromotive force of the motor shown in figure 23

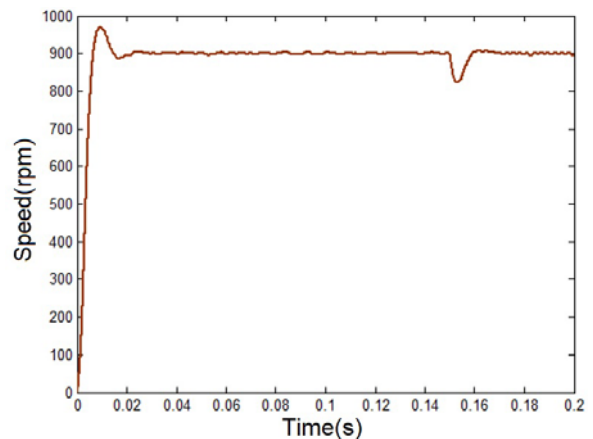


Fig.22. The motor speed

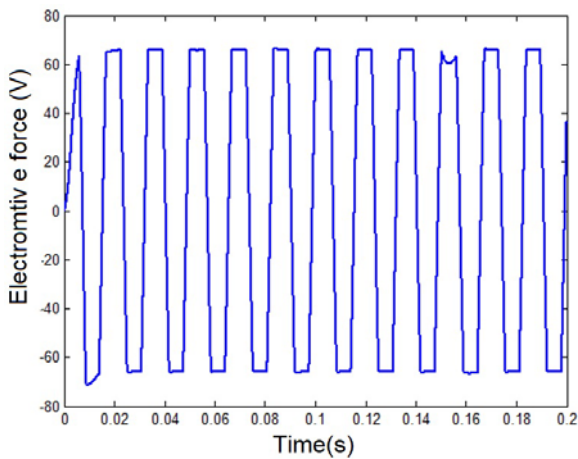


Fig.23. Electromotive force

Filtered: $L : 2e-3, C$
 Input voltage: 120V 60Hz
 Load: $t=0.15 T_m=4Nm$

5. Comparison between direct matrix converter and indirect converter

Table 2. Comparison Table

	DC/AC fed BLDC motor	Matrice converter fed BLDC motor
Conversion	DC/AC	AC/AC
Number of switches	6 unidirectional	09 bidirectional
Output signal quality	Good	Very good
The losses	Weak	practically weak
Exceeding the speed in transient mode	0%	7%
Speed overshoot after torque variation	3%	0%
THD	15%	2.88%
Torque exceeded in transient mode	9 N.m	18N.m
Torque overshoot after torque variation	7 N.m	5 N.m
The current overshoot after the variation	4A	2A

6. Conclusion

In this work we examines the impact of matrix converter and its ability to act as a variable speed drive attached to a BLDC motor.

The use of the matrix converter offers several advantages in terms of the quality of the motor currents and the minimization of overshoot during abrupt changes in torque.

However, in terms of cost, the classic inverter-based topology remains less expensive than the topology based on the indirect converter.

ACKNOWLEDGEMENTS

The authors are grateful for research funding from the General Direction of Scientific Research and Technological Development, DGRSDT.

REFERENCES

- [1] A. K. Singh and S. Pattnaik, "Matrix Converter Operated Hysteresis Current Controlled BLDC Motor Drive for Efficient Speed Control and Improved Power Quality," *Procedia Computer Science*, vol. 167, no. 2019, pp. 541–550, 2020, doi: 10.1016/j.procs.2020.03.314.
- [2] A. T. Hafez, A. A. Sarhan, and S. Givigi, "Brushless DC motor speed control based on advanced sliding mode control (SMC) techniques," *SysCon 2019 - 13th Annual IEEE International Systems Conference, Proceedings*, pp. 1–6, 2019, doi: 10.1109/SYSCON.2019.8836754.
- [3] D. Varajão and R. E. Araújo, "Modulation methods for direct and indirect matrix converters: A review," *Electronics (Switzerland)*, vol. 10, no. 7, pp. 1–29, 2021, doi: 10.3390/electronics10070812.
- [4] F. Pamuji, "Comparison of BLDC Motor Controller Design for Electric Vehicles Using Fuzzy Logic Controller and Artificial Neural Network," *Przegląd Elektrotechniczny*, vol. 1, no. 6, pp. 3–11, 2021, doi: 10.15199/48.2021.06.01.
- [5] M. Garcia et al., "Power Electronics for Drives Power Drives Lifetime Improved in Power Electronics Electronics Drives Lifetime Improved in Power Electronics for BLDC Drives using Fuzzy Logic and," *IFAC PapersOnLine*, vol. 52, no. 13, pp. 2372–2377, 2019, doi: 10.1016/j.ifacol.2019.11.561.
- [6] S. WONGKHEAD and S. TUNYASRIRUT, "Implementation of a dsp- tms320f28335 based state feedback with optimal design of pi controller for a speed of bldc motor by ant colony optimization," *Przegląd Elektrotechniczny*, vol. 97, no. 7, pp. 7–12, 2021, doi: 10.15199/48.2021.07.02.
- [7] E. Gowthaman, V. Vinodhini, M. Y. Hussain, S. K. Dhinakaran, and T. Sabarinathan, "ScienceDirect ScienceDirect 1st International Conference Assessing the feasibility of using temperature function a long-term demand forecast Speed Control of Permanent Magnet Brushless DC Motor Using Speed Control of Permanent ," *Energy Procedia*, vol. 117, pp. 1101–1108, 2017, [Online]. Available: <http://dx.doi.org/10.1016/j.egypro.2017.05.234>.
- [8] V. Mach, S. Kovář, J. Valouch, and M. Adámek, "Brushless DC motor control on arduino platform," *Przegląd Elektrotechniczny*, vol. 94, no. 11, pp. 105–107, 2018, doi: 10.15199/48.2018.11.24.
- [9] Y. Park, H. Kim, H. Jang, S. H. Ham, J. Lee, and D. H. Jung, "Efficiency Improvement of Permanent Magnet BLDC with Halbach Magnet Array for Drone," *IEEE Transactions on Applied Superconductivity*, vol. 30, no. 4, 2020, doi: 10.1109/TASC.2020.2971672.
- [10] M. Sumega, Š. Zoššák, P. Varecha, and P. Rafajdus, "Sources of torque ripple and their influence in BLDC motor drives," *Transportation Research Procedia*, vol. 40, pp. 519–526, 2019, doi: 10.1016/j.trpro.2019.07.075.
- [11] A. Popenda and M. Nowak, "Modelling of BLDC motor with different fashions of winding connection," *Przegląd Elektrotechniczny*, vol. 95, no. 2, pp. 92–95, 2019, doi: 10.15199/48.2019.02.21.
- [12] F. Korkmaz, I. Topaloglu, and H. Mamur, "DTC Control of BLAC and BLDC Motors for Pure Electric Vehicles," *International Journal of Instrumentation and Control Systems*, vol. 6, no. 2/3, pp. 9–17, 2016, doi: 10.5121/ijics.2016.6302.
- [13] D. Thiyarajan and B. Dora Arul Selvi, "Modified SVPWM based three phase to nine phase matrix converter for nine phase induction motor with closed loop speed control," *Journal of Ambient Intelligence and Humanized Computing*, vol. 12, no. 6, pp. 6091–6105, 2021, doi: 10.1007/s12652-020-02178-6.
- [14] J. Zhang, L. Li, D. G. Dorrell, M. Norambuena, and J. Rodriguez, "Predictive Voltage Control of Direct Matrix Converters with Improved Output Voltage for Renewable Distributed Generation," *IEEE Journal of Emerging and Selected Topics in Power Electronics*, vol. 7, no. 1, pp. 296–308, 2019, doi: 10.1109/JESTPE.2018.2874275.
- [15] H. F. Ahmed, H. Cha, and A. A. Khan, "A Single-Phase Buck Matrix Converter with High-Frequency Transformer Isolation and Reduced Switch Count," *IEEE Transactions on Industrial Electronics*, vol. 64, no. 9, pp. 6979–6988, 2017, doi: 10.1109/TIE.2017.2686329.
- [16] S. M. Dabour, A. S. Abdel-Khalik, S. Ahmed, A. M. Massoud, and S. M. Allam, "Common-mode voltage reduction for space vector modulated three- to five-phase indirect matrix converter,"

- International Journal of Electrical Power and Energy Systems, vol. 95, pp. 266–274, 2018, doi: 10.1016/j.ijepes.2017.08.020.
- [17] S. A. Rahman, S. B. Mule, E. D. Mitiku, G. T. Aduye, and C. Gopinath, "Highest voltage sag and swell compensation using single phase matrix converter with four controlled switches," *Przeglad Elektrotechniczny*, vol. 97, no. 4, pp. 134–138, 2021, doi: 10.15199/48.2021.04.24.
- [18] Z. Ortatepe and A. Karaarslan, "Error minimization based on multi-objective finite control set model predictive control for matrix converter in DFIG," *International Journal of Electrical Power and Energy Systems*, vol. 126, no. PA, p. 106575, 2021, doi: 10.1016/j.ijepes.2020.106575.
- [19] X. Dongxia, L. Shengmin, and S. Xuxia, "AC-AC Matrix Converter," 2009, pp. 205–208.
- [20] L. R. Merchan-Villalba, J. M. Lozano-Garcia, J. G. Avina-Cervantes, H. J. Estrada-Garcia, and J. Martinez-Patino, "Matrix Converter Based on SVD Modulation Using a Microcontroller as Unique Controlling Device," *IEEE Access*, vol. 7, no. November, pp. 164815–164824, 2019, doi: 10.1109/ACCESS.2019.2952380.
- [21] M. Boydak, A. Orhan, and A. Caliskan, "Using Buck-Boost Rectifier with Single-Phase-Matrix Converter to Reduce Switch Count Operation," 2020 7th International Conference on Electrical and Electronics Engineering, ICEEE 2020, pp. 111–115, 2020, doi: 10.1109/ICEEE49618.2020.9102479.
- [22] S. Ansari and A. Chandel, "Simulation based comprehensive analysis of direct and indirect matrix converter fed asynchronous motor drive," 2017 4th IEEE Uttar Pradesh Section International Conference on Electrical, Computer and Electronics, UPCON 2017, vol. 2018-Janua, pp. 9–15, 2017, doi: 10.1109/UPCON.2017.8251014.
- [23] M. Moghaddami, S. Member, A. I. Sarwat, and S. Member, "Single-Phase Soft-Switched AC-AC Matrix Converter with Power Controller for Bidirectional Inductive Power Transfer Systems," vol. 9994, no. c, pp. 1–11, 2018, doi: 10.1109/TIA.2018.2820640.
- [24] H. Boumediene, S. Hassaine, and B. Mazari, "Wielomianowe i nieliniowe sterowanie silnikiem indukcyjnym za pośrednictwem przetwornika macierzowego," *Przeglad Elektrotechniczny*, vol. 93, no. 11, pp. 133–139, 2017, doi: 10.15199/48.2017.11.29.
- [25] Q. H. Tran, T. D. Nguyen, and L. M. Phuong, "Simplified Space-Vector Modulation Strategy for Indirect Matrix Converter with Common-Mode Voltage and Harmonic Distortion Reduction," *IEEE Access*, vol. 8, no. Cmv, pp. 218489–218498, 2020, doi: 10.1109/ACCESS.2020.3042528.
- [26] M. Moghaddami and A. Sarwat, "Self-Tuned Single-Phase AC-AC Converter for Bidirectional Inductive Power Transfer Systems," pp. 1–6, 2017.
- [27] R. Wisniewski, G. Bazydło, P. Szczesniak, and M. Wojnakowski, "Petri net-based specification of cyber-physical systems oriented to control direct matrix converters with space vector modulation," *IEEE Access*, vol. 7, no. MC, pp. 23407–23420, 2019, doi: 10.1109/ACCESS.2019.2899316.
- [28] Z. Malekjamshidi, M. Jafari, J. Zhu, and D. Xiao, "Bidirectional power flow control with stability analysis of the matrix converter for microgrid applications," *International Journal of Electrical Power and Energy Systems*, vol. 110, no. March, pp. 725–736, 2019, doi: 10.1016/j.ijepes.2019.03.053.
- [29] A. Bento et al., "On the potential contributions of matrix converters for the future grid operation, sustainable transportation and electrical drives innovation," *Applied Sciences (Switzerland)*, vol. 11, no. 10, 2021, doi: 10.3390/app11104597.
- [30] G. Fink, *Power Systems*. 2017.
- [31] J. Zhang, L. Li, and D. G. Dorrell, "Control and applications of direct matrix converters: A review," *Chinese Journal of Electrical Engineering*, vol. 4, no. 2, pp. 18–27, 2018, doi: 10.23919/CJEE.2018.8409346.
- [32] L. Empringham, J. W. Kolar, J. Rodriguez, P. W. Wheeler, and J. C. Clare, "Technological issues and industrial application of matrix converters: A review," *IEEE Transactions on Industrial Electronics*, vol. 60, no. 10, pp. 4260–4271, 2013, doi: 10.1109/TIE.2012.2216231.
- [33] H. A. L. Id, "Modulation naturelle généralisée des convertisseurs matriciels pour la variation de vitesse To cite this version: HAL Id: tel-01128262 Modulation naturelle généralisée des convertisseurs matriciels pour la variation de," 2015.
- [34] H. N. Nguyen, M. K. Nguyen, V. Q. B. Ngo, T. T. Tran, J. H. Choi, and Y. C. Lim, "Input power factor compensation strategy for zero CMV-SVM method in matrix converters," *IEEE Access*, vol. 8, pp. 175805–175814, 2020, doi: 10.1109/ACCESS.2020.3025919.
- [35] M. P. Jati, E. Purwanto, and B. Sumantri, "Comparative study of indirect space vector and venturini modulation for matrix converter fed induction motor," *Journal of Physics: Conference Series*, vol. 1517, no. 1, pp. 1–8, 2020, doi: 10.1088/1742-6596/1517/1/012072.
- [36] H. N. Nguyen and H. H. Lee, "An Effective SVM Method for Matrix Converters with a Superior Output Performance," *IEEE Transactions on Industrial Electronics*, vol. 65, no. 9, pp. 6948–6958, 2018, doi: 10.1109/TIE.2017.2779438.
- [37] J. Muñoz-Castillo et al., "Design of the input and output filter for a matrix converter using evolutionary techniques," *Applied Sciences (Switzerland)*, vol. 10, no. 10, 2020, doi: 10.3390/app10103524.
- [38] H. She, H. Lin, X. Wang, and L. Yue, "Damped input filter design of matrix converter," *Proceedings of the International Conference on Power Electronics and Drive Systems*, pp. 672–677, 2009, doi: 10.1109/PEDS.2009.5385684.